J. Mater. Environ. Sci. 5 (3) (2014) 873-886
ISSN : 2028-2508
CODEN: JMESCN

Corrosion inhibition effect of 2,5-bis (3,4,5-trimethoxy phenyl)-1,3,4-oxadiazole (BTPO) on 18 Ni M250 grade welded maraging steel in 1.0 M sulphuric acid medium

Pradeep Kumar and A. Nityananda Shetty*
Department of Chemistry, National Institute of Technology Karnataka, Surathkal, Srinivasnagar - 575 025, Mangalore, Karnataka, India.

Received 25 June 2013, Revised 23 Feb 2014, Accepted 23 Feb 2014
** Corresponding author. E mail: nityashreya@gmail.com*

Abstract
Corrosion inhibition of welded maraging steel in 1.0 M sulphuric acid was studied in the presence of different concentrations of 2,5-bis (3,4,5-trimethoxy phenyl)-1,3,4-oxadiazole (BTPO) by electrochemical techniques. The results confided that BTPO was a good inhibitor, and the inhibition efficiencies obtained from potentiodynamic polarization and electrochemical impedance methods were in good agreement. The inhibitor, BTPO, acted essentially as a mixed-type inhibitor with its inhibition action through its surface adsorption. The inhibition effciency was found to increase with the increase in BTPO concentration but decreased with the increase in temperature. The activation parameters for the corrosion of the alloy and thermodynamic parameters for the adsorption of BTPO on the alloy surface were calculated and discussed. The adsorption of BTPO on welded maraging steel surface was predominantly through physisorption and obeyed the Langmuir adsorption isotherm. Scanning electron microscopy (SEM) and energy dispersive X-ray spectroscopy (EDS) study confirmed the formation of an anticorrosion protective film of BTPO on the metal surface.

Keywords: Maraging steel, BTPO, Corrosion rate, Inhibitor, EIS, SEM.

Introduction
The ultra-high strength materials of maraging steels are developed mainly for aerospace, aircraft and tooling applications [1]. These alloys derive their high strength from the age hardening of low carbon, Fe–Ni martensitic matrix [2]. This is a low carbon steel that classically contains about 18 wt % Ni, substantial amounts of Co and Mo, together with small additions of Ti. The alloys display good resistance to stress corrosion cracking and superior mechanical properties [3]. The remarkable property of being weldable in the solutionized condition followed by a low temperature (480°C) post weld maraging treatment makes these steels attractive for fabrication of large structures [4]. Corrosion of maraging steel is a fundamental academic and industrial alarm that has received a considerable amount of attention [5]. According to the available literature, atmospheric exposure of 18 Ni maraging steel leads to the corrosion of the alloy in a uniform manner and getting completely covered with the rust [6]. Maraging steels were found to be less susceptible to hydrogen embrittlement than common high strength steels due to the significantly low diffusion of hydrogen in them [7]. As used in variety of applications these steels frequently come in contact with corrosive environment. One of the strategies used to protect the metals from corrosion is to isolate the metal from the corrosive agents.

Application of corrosion inhibitors is the most economical and practical method to mitigate electrochemical corrosion. The adsorption of organic molecules at the metal/solution interface is of a great interest in surface science and can markedly change the corrosion resistance properties of metals. The efficiency of these molecules is mainly dependent on their ability to be adsorbed on the metal surface, which results with the replacement of water molecules at a corroding interface [8]. Most of the efficient inhibitors used in industry are organic compounds which mainly contain oxygen, sulphur, nitrogen atoms, and multiple bonds in their molecules, through which they are adsorbed on the metal surface [9-11]. It has been observed that many organic inhibitors usually promote the formation of a chelate on the metal surface, which includes the transfer of electrons from the organic compounds to metal forming coordinate covalent bond during such chemical

adsorption process [12]. The effectiveness of inhibition depends on the nature and surface charge of the metal, nature of the medium and chemical structure of the inhibitor such as functional groups, aromaticity, steric factor and electron density at the donor atoms [13]. There are only a few reports in the literature on the use of inhibitors in controlling the corrosion of maraging steel in acid solutions [14-17].

The objective of the present work is aimed at tracking a new organic inhibitor with good inhibition efficiency against the corrosion of welded maraging steel surface in sulphuric acid medium.

2. Experimental

2.1. Materials

The compositions of the welded maraging steel (18 Ni 250 grade) is as follows (wt %): C = 0.015%, Ni = 18%, Mo = 4.8 %, Co = 7 .75 %, Si = 0.1%, O = 30 ppm, H = 2.0 ppm, Ti = 0.45 %, Al = 0.005 - 0.15%, Mn = 0.1%, P = 0.01%, S = 0.01%, N = 30 ppm and the balance is Fe. The maraging steel plates of composition as mentioned above were welded by GTAW - DCSP (Gas tungsten arc welding - Direct-current straight polarity) using filler material of compositions: C = 0.015%, Ni = 17%, Mo = 2.55%, Co = 12%, Ti = 0.015%, Al = 0.4%, Mn = 0.1%, Si = 0.1% and the balance is Fe. The specimen was taken from the plates which are welded as per above.

2.2. Preparation of test coupons

The working specimen was cut from the plate and sealed with epoxy resin, leaving only 0.65 cm^2 of the surface area exposed to the electrolyte. Prior to each experiment, the working electrode was mechanically polished with fine grades of emery papers (400 - 2000 grade). Then it was degreased with acetone, washed with double distilled water and dried before immersing in the corrosion medium. All the experiments were carried out at different temperatures in the open atmosphere, under unstirred conditions. .

2.4. Synthesis of 2,5-bis (3,4,5-trimethoxy phenyl)-1,3,4-oxadiazole (BTPO)

To a mixture of 3,4,5-trimethoxy benzoic acid (0.05 mol) and 3,4,5-trimethoxy benzoic acid hydrazide (0.05 mol) phosphorous oxychloride was added drop wise. The mixture was refluxed on a water bath for 5 h. Then the reaction mixture was allowed to cool at room temperature and poured into crushed ice. The solid precipitated was filtered, dried and recrystallized from ethanol. The product was characterized by elemental analysis, melting point (207-208 °C) and infrared spectra [18].

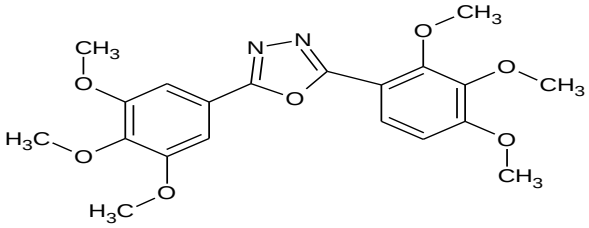

2,5-bis (3,4,5-trimethoxy phenyl)-1,3,4-oxadiazole

2.3. Medium

The corrosive medium was 1.0 M H_2SO_4 solution, prepared from analytical-reagent-grade 98% sulphuric acid and double distilled water. Inhibitive action of BTPO on the corrosion of welded maraging steel in 1.0 M H_2SO_4 solution was studied by introducing different concentrations of the inhibitor into the solution. The concentration range of BTPO prepared and used in this study was 0.2 mM - 1.0 mM. The experiments were carried out at temperatures 30 ℃, 35 ℃, 40 ℃, 45 ℃ and 50 ℃ (±0.5 ℃), in a calibrated thermostat

2.5. Electrochemical techniques

Electrochemical measurements were carried out by using an electrochemical work station, Gill AC having ACM instrument Version 5 software. The arrangement used was a conventional three - electrode compartment glass cell with a platinum counter electrode and a saturated calomel electrode (SCE) as reference. The working electrode was made of welded maraging steel. All the values of potential are referred to the SCE. The polarization studies were carried out immediately after the EIS studies on the same electrode without any further surface treatment.

2.5.1. Potentiodynamic polarization studies

Finely polished welded maraging steel specimen was exposed to the corrosion medium of 1.0 M sulphuric acid in the presence and absence of the inhibitor at different temperatures (30 – 50 ℃) and allowed to establish a steady-state open circuit potential (OCP). The potentiodynamic current - potential curves were recorded by polarizing the specimen to - 250 mV cathodically and +250 mV anodically with respect to the OCP at a scan rate of 1 mV s^{-1}.

2.5.2. Electrochemical impedance spectroscopy studies (EIS)

The impedance measurements were carried out in the frequency range of 10 KHz to 0.01 Hz, at the rest potential, by applying 10 mV sine wave AC voltage. The double layer capacitance (C_{dl}) and the charge transfer resistance (R_{ct}) were calculated from the Nyquist plots.

In all the above measurements, at least three similar results were considered, and their average values are reported.

2.6. SEM / EDS investigations

The surface topography of the welded maraging steel specimen immersed in 1.0 M H_2SO_4 solution in the presence and absence of inhibitor was compared by recording the SEM images of the samples using JEOL JSM - 6380LA analytical scanning electron microscopy. Energy dispersive X - ray spectroscopy (EDS) studies were carried out in order to identify the elemental composition of the species formed on the metal surface after its immersion in 1.0 M sulphuric acid in the presence and absence of the inhibitor.

3. Results and discussion

3.1. Potentiodynamic polarization measurements

Polarization curves for the corrosion of maraging steel in 1.0 M H_2SO_4 solution in the presence of different concentrations of BTPO are presented in Fig. 1. Electrochemical parameters such as corrosion potential (E_{corr}), corrosion current density (i_{corr}), and anodic and cathodic Tafel slopes (b_a, b_c) determined from the polarization measurements are listed in Table 1. It is usually assumed that the process of oxidation is uniform and does not occur selectively to any component of the alloy. The corrosion rate (υ_{corr}), in mm y^{-1}, is calculated from the following equation [19].

$$Corrosion\ rate\ (\upsilon_{corr}) = K\frac{i_{corr}}{\rho}EW \qquad (1)$$

where, K is a constant that defines the unit for the corrosion rate, i_{corr} is the current density in μA cm^{-2}, ρ is the density in g cm^{-3} and EW is the equivalent weight of the alloy. Equivalent weight of the alloy was calculated from the equation:

$$EW = \frac{1}{\Sigma\frac{n_i f_i}{W_i}} \qquad (2)$$

where, f_i is the mass fraction of the i^{th} element in the alloy, W_i is the atomic weight of the i^{th} element in the alloy and n_i is the valence of the i^{th} element in the alloy.

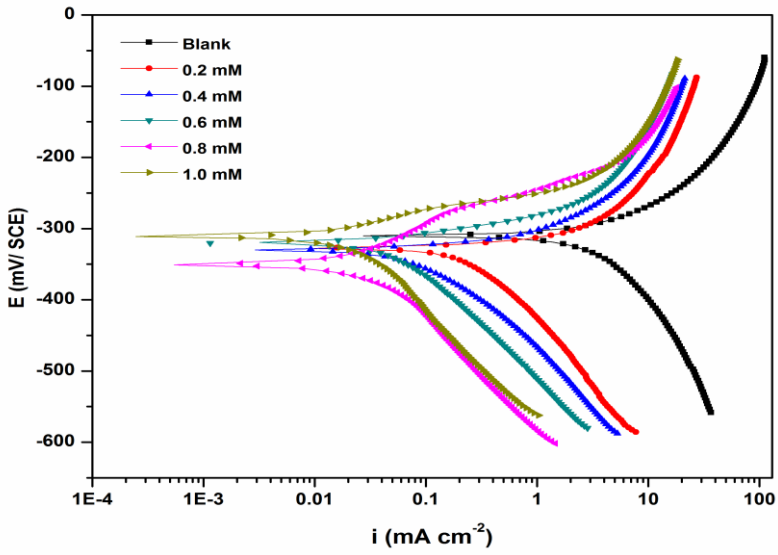

Figure 1: Tafel polarization curves for the corrosion of welded maraging steel in 1.0 M sulphuric acid containing different concentrations of inhibitor at 30 ℃.

The inhibition efficiency was calculated from the equation [20].

$$\eta(\%) = \frac{i_{corr} - i_{corr(inh)}}{i_{corr}} \times 100 \quad (3)$$

where, i_{corr} and $i_{corr(inh)}$ signify the corrosion current densities in the absence and presence of inhibitors, respectively.

It is observed from Fig. 1 and Table 1 that the corrosion current density (i_{corr}) decreases with the increase in the concentration of the inhibitor in the solution. The values of b_c and b_a change with the increase in the inhibitor concentration, indicating the influence of inhibitor concentration on the kinetics of both the cathodic and anodic reactions, i.e., hydrogen evolution and metal dissolution reaction, respectively. The presence of inhibitor does not cause any significant shift in the E_{corr} value. When the change in corrosion potential is more than ± 85 mV with respect to the corrosion potential of the blank, the inhibitor compound is considered as an exclusively anodic or a cathodic type inhibitor [21]. But the largest displacement of E_{corr} in the present study is about -38 mV, which implies that the inhibitor, BTPO, acts as a mixed type inhibitor, affecting both metal dissolution and hydrogen evolution reactions, but it is more predominant towards cathodic reaction [21].

Table 1: Results of potentiodynamic polarization studies on welded maraging steel in 1.0 M sulphuric acid containing different concentrations of BTPO

Temperature (℃)	Conc. of inhibitor (mM)	$-E_{corr}$ (mV /SCE)	b_a (mV dec^{-1})	$-b_c$ (mV dec^{-1})	i_{corr} (mA cm^{-2})	υ_{corr} (mm y^{-1})	η (%)
30	Blank	315	187	132	3.93	50.32	-
	0.2	334	148	124	0.87	11.21	77.9
	0.4	338	143	121	0.64	8.25	83.7
	0.6	322	139	117	0.48	6.19	87.8
	0.8	353	137	115	0.27	3.48	93.1
	1.0	312	132	112	0.23	2.96	94.1
35	Blank	313	198	147	4.21	54.12	-
	0.2	327	161	135	1.05	13.57	75.1
	0.4	310	157	129	0.80	10.31	80.9
	0.6	329	152	125	0.67	8.68	84.1
	0.8	334	149	122	0.51	6.51	87.8
	1.0	337	147	118	0.38	4.88	90.9
40	Blank	310	212	163	5.41	69.72	-
	0.2	324	183	149	1.68	21.62	68.9
	0.4	328	179	143	1.46	18.83	73.0
	0.6	331	175	139	1.19	15.34	78.0
	0.8	316	172	136	0.92	11.86	82.9
	1.0	305	164	134	0.70	9.07	87.1
45	Blank	312	243	178	6.70	86.36	-
	0.2	327	201	153	2.35	30.23	64.9
	0.4	318	192	148	2.08	26.77	68.9
	0.6	321	187	145	1.74	22.45	74.0
	0.8	332	183	141	1.47	19.00	78.1
	1.0	309	177	138	1.27	16.41	81.0
50	Blank	320	269	192	8.11	104.54	-
	0.2	318	214	174	3.33	42.86	58.9
	0.4	329	203	168	3.08	39.73	62.0
	0.6	333	195	164	2.76	35.54	65.9
	0.8	341	191	160	2.35	30.32	71.0
	1.0	352	183	157	2.11	27.18	73.9

The value of corrosion current density decreases with the increase in the inhibitor concentration indicating an increase in inhibition efficiency with the increase in inhibitor concentration. This can be attributed to the adsorption of BTPO on the alloy surface forming a barrier film at the interface between the metal and the corrosion medium. The BTPO film formed on the metal surface reduces the probability of both the anodic and cathodic reactions, which results in the decrease in corrosion rate [22]. The extent of adsorption increases with the increase in the concentration of BTPO; increasing the surface coverage on the alloy, accounting for the decrease in the corrosion rate.

3.2. Electrochemical Impedance Spectroscopy (EIS)

To examine the characteristics and kinetics of the electrochemical processes on the welded maraging steels in H_2SO_4 solutions, electrochemical impedance measurements were carried out in the presence of different concentrations of BTPO. Nyquist plots for the corrosion of welded maraging steel in 1.0 M H_2SO_4 solution in the presence of different concentrations of BTPO are given in Fig. 2. The impedance parameters calculated from the plots are summarised in Table 2. It can be observed from Fig. 2 that the diameter of the semicircle in the Nyquist plot increases, indicating an decrease in the corrosion rate with the increase in BTPO concentration. The impedance spectra shown in Fig. 2 do not present perfect semicircles. The distortions observed in the Nyquist plots are attributed to the frequency dispersion [14] due to the surface inhomogeneity.

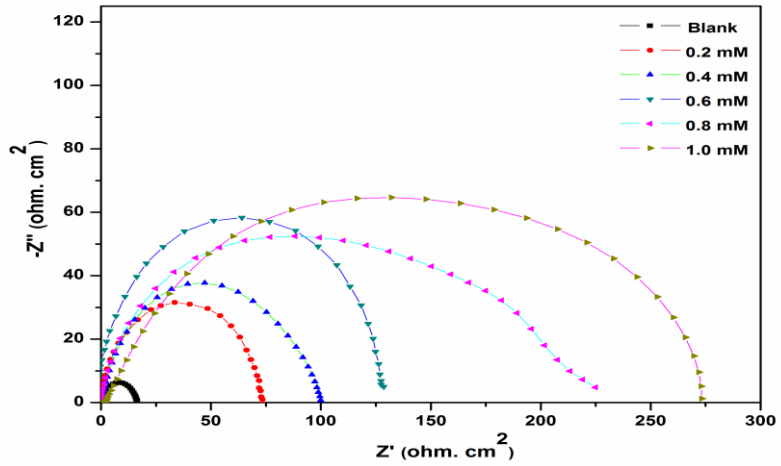

Figure 2: Nyquist plots for the corrosion of welded maraging steel specimen in 1.0 M sulphuric acid containing different concentrations of inhibitor at 30 ℃.

The Nyquist plot for the corrosion of the alloy in the absence of BTPO showed a single semicircle capacitive loop, which is attributable to the interfacial charge transfer of the corrosion process [23-25]. The circuit fitment was done by ZSimpWin software of version 3.21. The standard 'Randles' circuit model was used and is shown in Fig. 3(a), which consists of the electrolyte resistance (R_s), charge transfer resistance (R_{ct}) and double layer capacitance (C). The constant phase element, CPE, is substituted for the ideal capacitive element to give a more accurate fit to account for the depressed nature of the semicircles.

The *CPE* impedance (Z_{CPE}) is given by the expression:

$$Z_{CPE} = \frac{1}{Q} \times \frac{1}{(j\omega)^n} \qquad (4)$$

where, Q is the *CPE* coefficient, n is the *CPE* exponent (phase shift), ω is the angular frequency in rad s^{-1} and j is the imaginary unit ($j^2 = -1$). The value of CPE exponent n is given by ($-1 \leq n \leq 1$), the *CPE* simulates an ideal double-layer capacitor when n = 1 (C_{dl}), an ideal inductor for n = –1, and an ideal resistor for n = 0. The correction of capacitance to its real values is calculated from the following expression [26]:

$$C_{dl} = Q(\omega_{max})^{n-1} \qquad (5)$$

where, ω_{max} is the frequency at which the imaginary part of impedance ($-Z_i$) has a maximum.

Table 2: EIS data of welded maraging steel in 1.0 M sulphuric acid containing different concentrations of BTPO

Temperature (℃)	Conc. inhibitor (mM)	R_{ct} (ohm. cm^2)	C_{dl} (mF cm^{-2})	η (%)
30	Blank	16.1	0.69	-
	0.2	69.3	0.57	76.7
	0.4	97.4	0.54	83.5
	0.6	126.9	0.51	87.3
	0.8	214.2	0.46	92.4
	1.0	262.7	0.43	93.8
35	Blank	13.5	0.71	-
	0.2	52.1	0.62	74.1
	0.4	68.5	0.59	80.3
	0.6	78.0	0.57	82.7
	0.8	106.2	0.52	87.3
	1.0	123.8	0.51	89.1
40	Blank	10.4	0.67	-
	0.2	33.2	0.65	68.7
	0.4	36.6	0.63	71.6
	0.6	44.1	0.61	76.4
	0.8	59.0	0.58	82.4
	1.0	75.9	0.55	86.3
45	Blank	8.6	0.87	-
	0.2	24.3	0.71	64.7
	0.4	29.5	0.68	70.9
	0.6	32.8	0.66	73.8
	0.8	41.1	0.63	79.1
	1.0	51.8	0.60	83.4
50	Blank	7.3	1.12	-
	0.2	18.2	1.03	60.1
	0.4	19.1	0.92	61.8
	0.6	21.5	0.84	66.1
	0.8	25.0	0.79	70.8
	1.0	27.9	0.76	73.9

The impedance plots recorded for the corrosion of welded maraging steel in 1.0 M H_2SO_4 solution in the presence of BTPO are modelled by using the equivalent circuit depicted in Fig. 3(b), which consists of the R_s, CPE(Q), R_{ct}, R_f (film resistance) and C (film capacitance). The film resistance and film capacitance appear due to the adsorption and film formation by the inhibitor molecules on the surface of the alloy.

(a) **(b)**

Figure 3: Equivalent circuit used to fit the experimental EIS data for the corrosion of welded maraging steel specimen in 1.0 M sulphuric acid at 30 ℃ (a) for the blank solution and (b) in the presence of inhibitor.

It is evident from the data in Table 2 that the double layer capacitance decreases with the increase in the concentration of BTPO and the same can be attributed to the gradual replacement of adsorbed water molecules at metal/solution interface by the adsorption of the BTPO molecules, which is leading to an anticorrosion film

on the metal surface [27]. In addition, the more the inhibitor is adsorbed, the more the thickness of the barrier layer, decreasing the C_{dl} value, in accordance to the following expression of the Helmholtz model [28].

$$C_{dl} = \frac{\varepsilon\varepsilon_o}{d} S \quad (6)$$

where, d is the thickness of the film, S is the surface area of the electrode, ε_o is the permittivity of the air, and ε is the local dielectric constant.

The R_{ct} was used to calculate the inhibition efficiency ($\eta\%$) as per the following equation [29]:

$$\eta(\%) = \frac{R_{ct(inh)} - R_{ct}}{R_{ct(inh)}} \times 100 \quad (7)$$

The phase angle Bode plots for the corrosion of welded maraging steel in the presence of different concentrations of BTPO are shown in Fig. 4. The phase angle increases with the increase in the concentrations of BTPO in the sulphuric acid medium. This is due to the decrease in the dissolution of the alloy and decrease in the capacitive behaviour on the electrode surface.

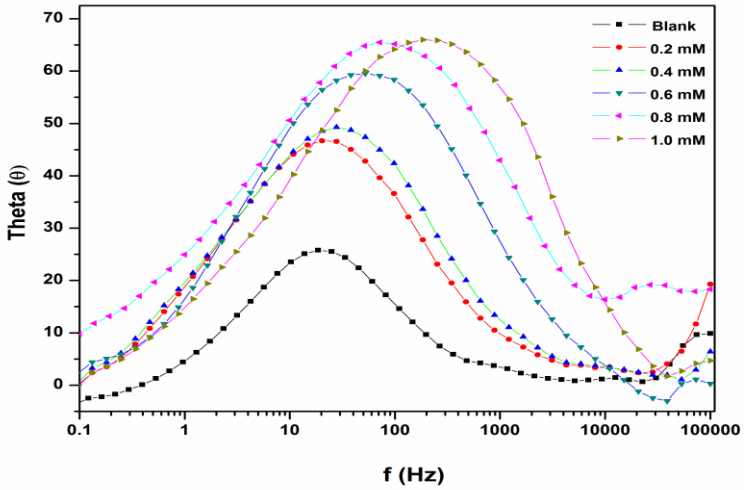

Figure 4: Bode plots for the corrosion of welded maraging steel specimen in 1.0 M sulphuric acid containing different concentrations of inhibitor at 30 ℃.

3.3. Effect of temperature

The results of potentiodynamic polarization and electrochemical impedance spectroscopy studies given in Tables 1-2 indicate that the inhibition efficiency of BTPO decreases with the increase in temperature. It is evident from the data in the Tables 1 and 2 that, with the increase in solution temperature, corrosion potential (E_{corr}), anodic Tafel slope (b_a), and cathodic Tafel slope (b_c) values do not change significantly. This indicates that the increase in temperature does not change the mechanism of corrosion reaction. However, i_{corr} and hence the corrosion rate of the specimen increase with the increase in temperature in both the blank and the inhibited solutions. The decrease in the inhibition efficiency with the increase in temperature may be attributed to the higher dissolution rates of the alloy at elevated temperatures and also to a possible desorption of adsorbed inhibitor due to increased solution agitation resulting from higher rates of hydrogen reduction. The rapid evolution of hydrogen on the alloy surface may also reduce the ability of the inhibitor molecules to be adsorbed on the metal surface. The decrease in R_{ct} and inhibition efficiency with the increase in temperature indicates desorption of the inhibitor molecules from the metal surface on increasing the temperature. This fact is also suggestive of physisorption of the inhibitor molecules on the metal surface [30]. In acidic medium, the corrosion rate increases exponentially with temperature increase because the hydrogen evolution overpotential decreases [31].

The apparent activation energy (E_a) for the corrosion process in the presence and absence of inhibitor can be calculated using Arrhenius law Equation [27].

$$\ln(\upsilon_{corr}) = B - \frac{E_a}{RT} \quad (8)$$

where, B is a constant which depends on the metal type, R is the universal gas constant and T is the absolute temperature. The plot of $ln(\upsilon_{corr})$ versus reciprocal of absolute temperature ($1/T$) gives a straight line with slope = - E_a / R, from which, the activation energy values for the corrosion process were calculated. The Arrhenius plots for the corrosion of welded maraging steel in the presence of different concentrations of BTPO in 1.0 M H_2SO_4 are shown in Fig. 5.

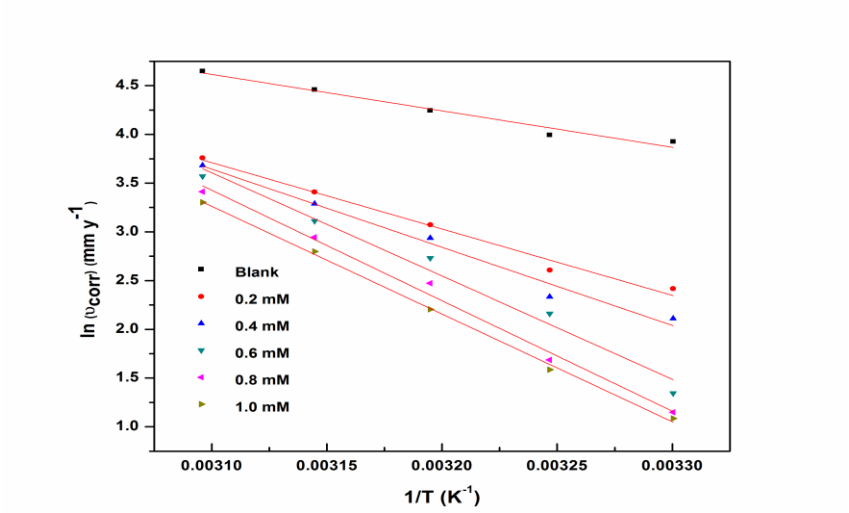

Figure 5: Arrhenius plots for the corrosion of welded maraging steel in 1.0 M sulphuric acid containing different concentrations of inhibitor.

The enthalpy of activation ($\Delta H^{\#}$) and entropy of activation ($\Delta S^{\#}$) for the corrosion of alloy were calculated from the transition state theory relation [27].

$$\upsilon_{corr} = \frac{RT}{Nh}\exp\left(\frac{\Delta S^{\#}}{R}\right)\exp\left(\frac{-\Delta H^{\#}}{R}\right) \quad (9)$$

where, h is Plank's constant, and N is Avagadro's number. The plots of $ln(\upsilon_{corr}/T)$ versus $1/T$ for the corrosion of welded maraging steel in the presence of different concentrations of BTPO in 1.0 M H_2SO_4 are shown in Fig. 6. The calculated values of E_a, $\Delta H^{\#}$ and $\Delta S^{\#}$ are presented in Table 3.

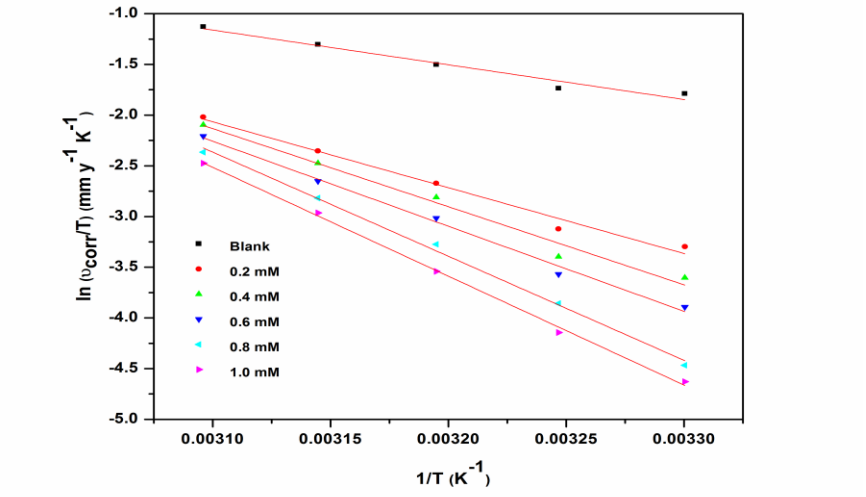

Figure 6: Plots of ln(υ_{corr}/T) versus 1/T for the corrosion of welded maraging steel in 1.0 M sulphuric acid containing different concentrations of inhibitor.

The data in the Table 3 show that the activation energy values (E_a) for the corrosion of welded maraging steel in 1.0 M H_2SO_4 in the presence of BTPO is higher than those in the uninhibited medium. The increase in the E_a values, with the increase in the inhibitor concentration indicates the increase in the energy barrier for the corrosion reaction, with the increasing concentrations of the inhibitor [32]. It is also observed that the whole process is controlled by surface reaction, since the activation energies of the corrosion process are above 20 kJ mol^{-1}. The adsorption of the inhibitor on the electrode surface leads to the formation of an barrier layer between the metal surface and the corrosion medium, blocking the charge transfer, and thereby reducing the metal reactivity in the electrochemical reactions of corrosion. The decrease in the inhibition efficiency of BTPO with the increase in temperature can be considered due to the decrease in the extent of adsorption of the inhibitor on the metal surface with the increase in temperature, and corresponding increase in corrosion rate as a greater area of the metal surface is exposed to the corrosion medium. The observations also support the view that the inhibitor is adsorbed on the metal surface through physisorption [30].

Table 3: Activation parameters for the corrosion of welded maraging steel in 1.0 M sulphuric acid containing different concentrations of inhibitor

Conc. of inhibitor (mM)	E_a (kJ^{-1} mol^{-1})	$\Delta H^{\#}$ (kJ^{-1} mol^{-1})	$\Delta S^{\#}$ (J mol^{-1} K^{-1})
Blank	31.08	29.46	-115.68
0.2	56.61	54.01	-47.31
0.4	66.64	64.04	-16.79
0.6	88.13	69.77	-0.12
0.8	94.23	85.38	47.36
1.0	91.89	89.28	58.25

The negative values of entropy of activation ($\Delta S^{\#}$) for the corrosion process imply that the activated complex in the rate determining step represents an association rather than dissociation, resulting in a decrease in randomness on going from the reactants to the activated complex [29]. Entropy of activation increases with the increase in the inhibitor concentration.

3.4. Adsorption isotherm

The inhibition action of organic inhibitors are generally through their adsorption on the metal/alloy surfaces. The phenomenon of adsorption of the inhibitor depends upon number of factors such as the charge and the nature of the metal surface, electronic properties of the metal surface on adsorption of solvent and other ionic species, temperature of the corrosion reaction and the electrochemical potential at the metal solution interface [33]. The adsorption of BTPO molecules on the metal surface can occur either through donor-acceptor interaction between the unshared electron pairs and/or π electrons of inhibitor molecule and the vacant d-orbitals of the metal surface atoms, or through electrostatic interaction of the inhibitor molecules with already adsorbed sulphate ions. The adsorption isotherms provide important clues about the nature of the metal-inhibitor interaction. The adsorption of an organic adsorbate at metal/solution interface can be presented as a substitution adsorption process between the inhibitor molecules in aqueous solution ($Inh_{(sol)}$), and the water molecules on metallic surface, (H_2O_{ads}) as given below [34].

$$Inh_{(sol)} + \chi H_2O_{(ads)} \leftrightarrow Inh_{(ad)} + \chi H_2O_{(sol)} \quad (10)$$

where,χ, the size ratio, is the number of water molecules displaced by one molecule of the adsorbate inhibitor. Inhibitor molecules adsorb on the metal surface if the interaction between the molecules and the metal surface is greater than that of the water molecule and the metal surface [35].

The surface coverage values (θ) were determined graphically by fitting a suitable adsorption isotherm to explain the behaviour associated with the experimental results. Among these models, the Langmuir model provides a good fit. The Langmuir adsorption isotherm is represented as follows:

$$\frac{C_{inh}}{\theta} = C_{inh} + \frac{1}{K} \quad (11)$$

where, K is the adsorption/desorption equilibrium constant, C_{inh} is the corrosion inhibitor concentration in the solution, and θ is the surface coverage, which is calculated using equation [29].

$$\theta = \frac{\eta(\%)}{100} \quad (12)$$

where, $\eta(\%)$ is the percentage inhibition efficiency. The plots of C_{inh}/θ versus C_{inh} gives a straight line with an intercept of $1/K$. The Langmuir adsorption isotherms for the adsorption of BTPO on the maraging steel surface are shown in Fig. 7.

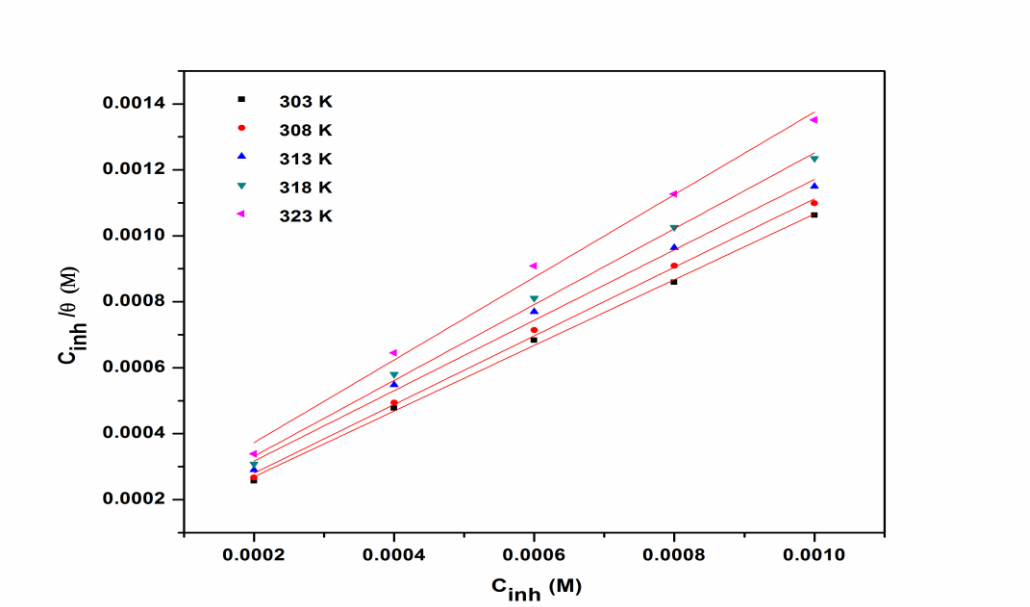

Figure 7: Langmuir adsorption isotherms for the adsorption of BTPO on welded maraging steel in 1.0 M sulphuric acid at different temperatures.

The values of standard free energy ΔG^0_{ads} of adsorption are related to K by the relation [36].

$$K = \frac{1}{55.5}\exp\left(\frac{-\Delta G^0_{ads}}{RT}\right) \quad (13)$$

where, the value 55.5 is the concentration of water in solution in mol dm^{-3}, R is the universal gas constant and T is absolute temperature. Standard enthalpy of adsorption (ΔH^0_{ads}) and standard entropies of adsorption (ΔS^0_{ads}) were obtained from the plot of (ΔG^0_{ads}) versus T according to the thermodynamic equation [20].

$$\Delta G^0_{ads} = \Delta H^0_{ads} - T\Delta S^0_{ads} \quad (14)$$

The thermodynamic data obtained are tabulated in Table 4.

Table 4: Thermodynamic parameters for the adsorption of BTPO on welded maraging steel surface in 1.0 M sulphuric acid at different temperatures

Temperature (° C)	$-\Delta G^o_{ads}$ (kJ mol^{-1})	ΔH^o_{ads} (kJ mol^{-1})	ΔS^o_{ads} (J mol^{-1} K^{-1})
30	34.21	-22.76	-37.6
35	34.35		
40	34.43		
45	34.69		
50	34.98		

The spontaneity of the adsorption of BTPO molecules on the alloy surface is indicated by the negative values of ΔG^0_{ads}. Generally the values of ΔG^0_{ads} less negative than -20 kJ mol^{-1} are attributed to a physisorption process, while more negative values than - 40 kJ mol^{-1} are attributed to a chemisorptions process [37]. The ΔG^0_{ads} values in the range of 34 – 35 kJ mol^{-1} in the present case indicates a mixed adsorption of BTPO molecules, through both physisorption and chemisorptions on the alloy surface. The enthalpy of adsorption value of -22.76 kJ mol^{-1} is suggestive of a physisorption process on the alloy surface. The decrease in the

inhibition efficiency with the increase in temperature also supports the view that the adsorption of BTPO on the alloy surface is physisorption. Therefore it can be concluded that the adsorption of BTPO on the alloy surface is through mixed adsorption with predominant physisorption.

3.5. Mechanism of corrosion inhibition

The mechanism of corrosion inhibition by a specific inhibitor is dependent on the adsorption of the inhibitor molecules on the metal surface, and their action in retarding the corrosion reaction as a whole. The mechanism of inhibition can be predicted from the knowledge of the interaction between the inhibitor molecules and the surface of the metal. According to the mechanism for the dissolution of iron in acidic sulphate solution initially proposed by Bockris et al. and Obot et al., iron dissolution in acidic sulphate solution depends initially on the adsorbed intermediate as follows [38].

$$Fe + H_2O \leftrightarrow FeOH_{ads} + H^+ + e^-$$

$$FeOH_{ads} \rightarrow FeOH^+ + e^- \text{ (rate determining step)}$$

$$FeOH^+ + H^+ \leftrightarrow Fe^{2+} + H_2O$$

The cathodic hydrogen evolution follows the steps

$$Fe + H^+ \leftrightarrow (FeH^+)_{ads}$$

$$(FeH^+)_{ads} + e^- \leftrightarrow (FeH)_{ads}$$

$$(FeH)_{ads} + H^+ + e^- \rightarrow Fe + H_2$$

$$(FeH)_{ads} + (FeH)_{ads} \rightarrow 2Fe + H_2$$

The following mechanism involving two adsorbed intermediates to account for the retardation of Fe anodic dissolution in the presence of an inhibitor:

$$Fe + H_2O \leftrightarrow FeH_2O_{ads}$$

$$FeH_2O_{ads} + I \leftrightarrow FeoH^-_{ads} + H^+ + I$$

$$FeH_2O_{ads} + I \leftrightarrow FeI_{ads} + H_2O$$

$$FeOH^-_{ads} \rightarrow FeOH_{ads} + e^- \text{ (rate determining step)}$$

$$FeI_{ads} \leftrightarrow FeI^+_{ads} + e^-$$

$$FeOH_{ads} + FeI^+_{ads} \leftrightarrow FeOH^+ + FeI_{ads}$$

$$FeOH^+ + H^+ \leftrightarrow Fe^{2+} + H_2O$$

where, I represents the inhibitor species. According to the above detailed mechanism, displacement of some adsorbed water molecules on the metal surface by inhibitor species to yield the adsorbed intermediate FeI_{ads}, which reduces the amount of the species $FeOH^-_{ads}$ available for the rate determining steps and consequently retards metal dissolution.

The adsorption mechanism of a specific inhibitor depend on factors such as the behaviour of the metal, temperature, the conductive medium, pH, and the inhibitor concentration, and the functional groups present in the molecule as different groups are adsorbed to different degrees. As reported in the literature [24], the surface charge of iron in sulphuric acid solution at the free corrosion potential is positive. Therefore, the negatively charged sulphate ions in the solution are adsorbed on the metal surface through electrostatic interaction resulting in physisorption. In the study of the effect of inorganic anions and organic compounds on corrosion inhibition of mild steel in various acids, Hackerman et al. [39] have reported that the degree of adsorption of anions was in the order $I^- > Br^- > Cl^- > SO_4^{2-} > ClO_4^-$. The sulphate ions with low degree of adsorption could not cover the metal surface fully and therefore there is always possibility of the inhibitor molecules occupying the vacant adsorption sites on the metal surface via physisorption through electrostatic interaction through their electron rich centres via the chemisorptions. The possible bonding sites of the inhibitor are the free electron pairs on nitrogen and oxygen atoms. The neutral inhibitor molecules can also adsorb via chemosorption on the vacant sites on the metal surface through the free electron pairs on nitrogen atoms, as well as oxygen, which could interact with vacant d orbital of iron [40]. As the inhibitor molecule is bulkier, they spread over the metal surface, effectively covering the metal surface and protecting it from corrosion.

3.6. SEM / EDS Studies

In order to differentiate between the surface morphology and to identify the composition of the species formed on the metal surface after its immersion in 1.0 M H_2SO_4 in the absence and the presence of BTPO, SEM/EDS investigations was carried out. Fig. 9(a) represents the SEM image of the corroded welded maraging steel sample. The corroded surface shows separation of the particles from the surface. The corrosion of welded alloy may be predominantly attributed to the inter-granular corrosion assisted by the galvanic effect between the precipitates and the matrix along the grain boundaries. Fig.9(b) represents SEM image of welded maraging steel after the corrosion tests in a medium of sulphuric acid containing 1.0 mM of BTPO. The image clearly shows the relatively smooth surface of the alloy. The adsorbed inhibitor layer protects the metal from corrosion. EDS investigations were conducted in order to identify the species composition formed on the metal surface after immersion in 1.0 M sulphuric acid in the absence and presence of BTPO.

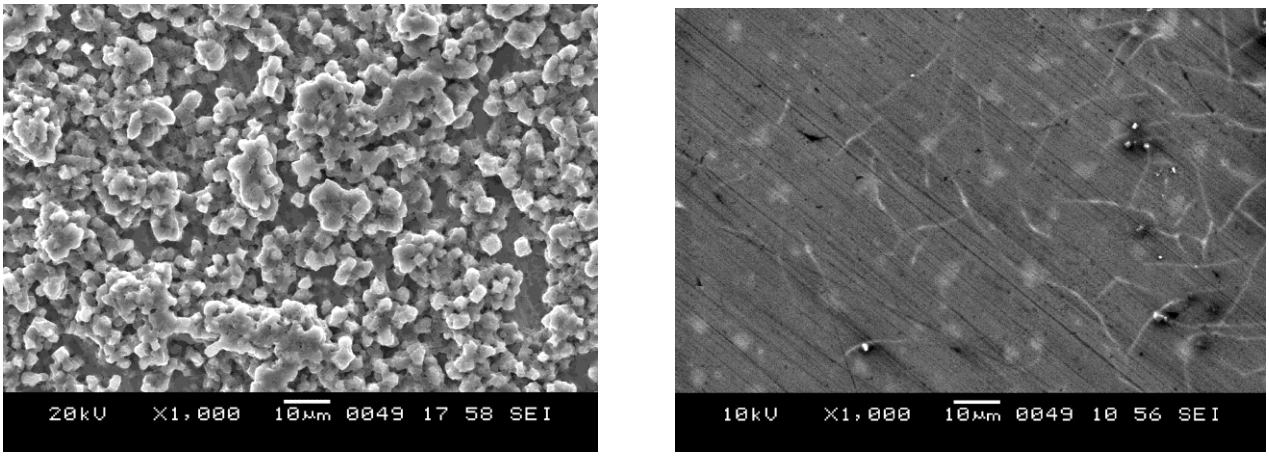

(a) (b)

Figure 8: SEM images of the welded maraging steel after immersion in 1.0 M sulphuric acid a) in the absence and b) in the presence of BTPO

The corresponding EDS profile analyses for the selected areas on the SEM images 9(a) and 9(b) are shown in Fig. 10(a) and Fig. 10(b), respectively. The atomic percentages of the elements found in the EDS profile for corroded metal surface were 21.36 % Fe, 5.51% Ni, 12.47% Mo, 45.87% O, 3.17 % Co and 11.62% S and suggested that formation of metal oxides. These elemental compositions prove that oxidation of metallic elements in the presence of acidic solution. The atomic percentages of the elements found in the EDS profile for inhibitor adsorbed metal surface were 9.42 % Fe, 2.02% Ni, 2.05% Mo, 47.82% O, 10.64% N, 13.30% C and 14.66% S and suggested that formation of anticorrosion protective film by the inhibitor.

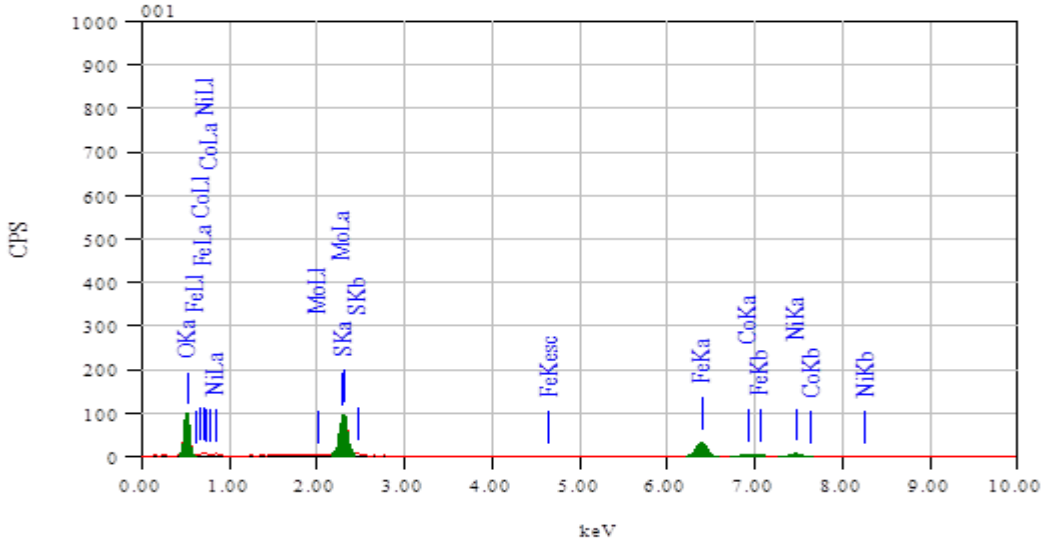

(a)

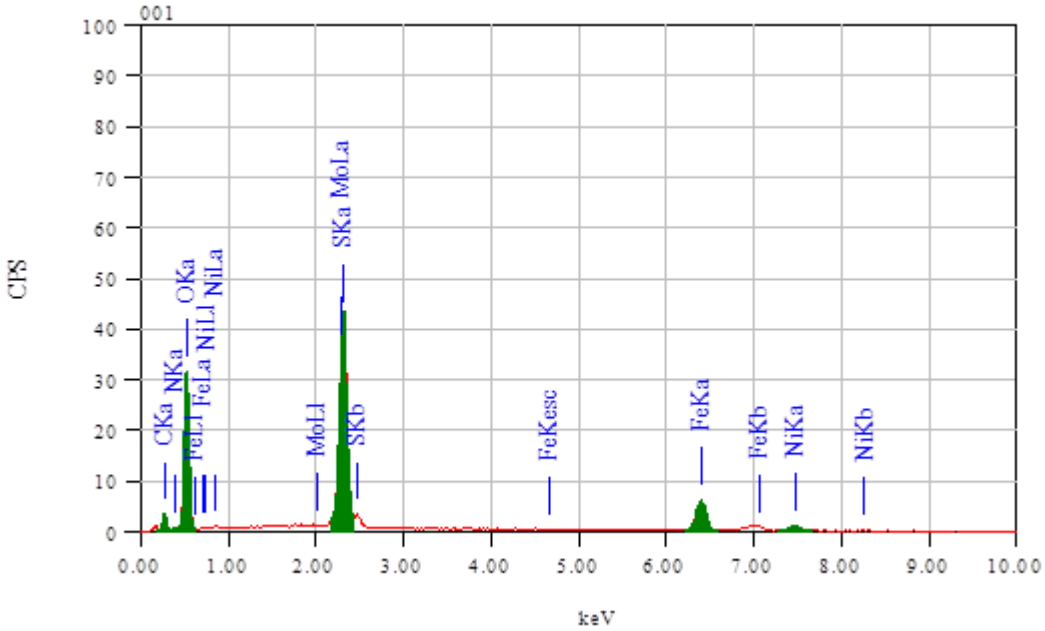

(b)

Figure 9: EDS spectra of the welded maraging steel after immersion in 1.0 M sulphuric acid a) in the absence and b) in the presence of BTPO

Conclusions

- The BTPO acts as a mixed type inhibitor for the corrosion of welded maraging steel in sulphuric acid solution, affecting both the anodic dissolution and hydrogen evolution reactions.
- The inhibition efficiency of BTPO increases with the increase in its concentration and decreases with the increase in temperature.
- The adsorption of BTPO was found to be predominantly through physical adsorption and follows the Langmuir's adsorption isotherm.
- The results obtained from EIS and polarization studies are in a good agreement.

References

1. ASM handbook, vol. 1. ASM International, Materials Park, OHIO, USA, 2005.
2. Rohrbach K., Schmidt M., ASM Handbook, 10th ed., vol. 1, ASM International, 1990.
3. Tsay L. W., Chen H. H., Chiang M. F., Chen C., *Corros. Sci.* 49 (2007) 2461.
4. Adama C. M., Travis R. E., *Weld. J.* 43 (1964) 193.
5. Uhlig H. H., Revie R. W., Corrosion and Corrosion Control; Wiley: New York, 1985.
6. Krick W. W., Covert R. A., May T. P., *Met. Eng. Quart.* 8 (1968) 31.
7. Rezek J., Klein I. E., Yhalom J., *Corros. Sci.* 39 (1999) 385.
8. Bockris J. O. M., Reddy A. K. N., Modern Electrochemistry, vol. 2, Plenum Publishing Corporation, 227 West 17th, Street, New York, 1976.
9. Gomez B., Likhhanova N. V., Dominguez-Aguilar M. A., Martinez-Palou R., Vela A., Gazquez J. L., *J. Phys. Chem. B.* 110 (2006) 8928.
10. Abdulwahab M., Kasim A., Fayomi O. S. I., Asuke F., Popoola A. P. I., *J. Mater. Environ. Sci.* 3 (2012) 1177 - 1182.
11. Prabakaran M., Vadivu K., Ramesh S., Periasamy V., *J. Mater. Environ. Sci.* 5 (2014) 553 - 564.
12. Fang J., Li J. J., *Mol. Struct.* 593 (2002) 179.
13. Tamil Selvi S., Raman V., Rajendran N., *J. Appl. Electrochem.* 33 (2003) 1175.
14. Poornima T., Nayak J., Shetty A. N., *J. Appl. Electrochem.* 41 (2011) 223.
15. Poornima T., Nayak J., Shetty A. N., *Corros. Sci.* 53 (2011) 3688.
16. Sanathkumar B. S., Nayak J., Shetty A. N., *J. Coat. Technol. Res.* 9 (2012) 483.
17. Sanathkumar B. S., Nayak J., Shetty A. N., *Int. J. Hydrogen Energy*, 37 (2012) 9431.
18. Mazzone G., Bonina F., Puglisi G., Panico A. M., Arrigo Reina R., *Farmaco-Ed. Sci.* 39 (1984) 414.
19. Dean S. W., Norm ASTM G102. Standard practice for calculation of corrosion rates and related information from electrochemical measurements. 1999.

20. Prabhu R. A., Shanbhag A. V., Venkatesha T. V., *J. Appl. Electrochem.* 37 (2007) 491.
21. Jayaperumal D., *Mater. Chem. Phys.* 119 (2010) 478.
22. Li W., He, Q., Zhang S., Pei C., Hou B. J., *Appl. Electrochem.* 38 (2008) 289.
23. Tao Z., Zhang S., Li W., Hou B., *Corros. Sci.* 51 (2009) 2588.
24. Popova A., Sokolova E., Raicheva S., Christov M., *Corros. Sci.* 45 (2003), 33.
25. Ashassi-Sorkhabi H., Ghalebsaz-Jeddi N., Hashemzadeh F., Jahani H., *Electrochim. Acta* 51 (2006) 3848.
26. Machnikova E., Whitmire H. K., Hackerman N., *Electrochim. Acta*. 53 (2008) 6024.
27. Bentiss F., Lebrini M., Lagrenee M., *Corros. Sci.* 47 (2005) 2915.
28. Hassan H. H., *Electrochim. Acta* 51 (2006) 5966.
29. Wang X., Yang H., Wang F., *Corros. Sci.* 52 (2010) 1268.
30. Geetha M. P., Nayak J., Shetty A. N., *Mater. Chem. Phys.* 125 (2011) 628.
31. Obi-Egbedi N. O., Obot I. B., *Corros. Sci.* 53 (2011) 263.
32. Avci G., *Colloids Surf., A* 317 (2008) 730.
33. Villamil R. F. V., Corio P., Agostinho S. M. L., Rubin J. C. J., *Electroanal. Chem*. 472 (1999) 112.
34. Moretti G., Quartarone G., Tassan A., Zingales A., *Mater. Corros.* 45 (1994), 641.
35. Tao Z., Zhang S., Li W., Hou B., *Ind. Eng. Chem. Res.* 49 (2010) 2593.
36. Fekry A. M., Ameer M. A., *Int. J. Hydrogen Energy* 35 (2010) 7641.
37. Singh A. K., Quraishi M. A., *Corros. Sci.* 53 (2011) 1288.
38. Obot I. B., Obi-Egbedi N. O., Eseola A. O., *Ind. Eng. Chem. Res.* 50 (2011) 2098.
39. Hackerman N., Snavely E. S. Jr,. Payne J. S. Jr., *J. Electrochem Soc.* 113 (1966) 677.
40. Satpati A. K., Ravindran P. V., *Mater. Chem. Phys.* 109 (2008) 352.